Inertial Particle Behavior in an Unsteady Separated Flow

G. B. Jacobs *
Department of Aerospace Engineering & Engineering Mechanics,
San Diego State University,
5500 Campanile Drive, San Diego, CA, 92182.

A new inertial particle behavior is identified in a particle-laden, unsteady separated flow behind a backward-facing step. In a numerical investigation, it is shown that inertial particles eject away from the wall along a distinct material line that originates from a fixed wall location. The fixed separation location coincides with the zero averaged wall skin friction location of the carrier flow. At Stokes numbers larger than one, inertial particles separate at moderate angles. At Stokes numbers smaller than one, the inertial particle dispersion compares to the fluid particle traces showing a moving separation origin of the material line. The Saffman lift forces particles away from the wall and pollutes the distinct character of the separation material line.

Nomenclature

A_c	particle relative acceleration
c_p	$\frac{p-p_\infty}{\rho u_\infty^2/2}$ pressure coefficient
C_p	specific heat of the fluid
C_A	virtual mass correction factor for high Reynolds numbers
C_{Ds}	Stokes drag correction factor for high Reynolds numbers
C_H	Basset history correction factor for high Reynolds numbers
d_d	particle diameter
e	energy flux
F	flux vector in x-direction
G	flux vector in y-direction
L_f	reference length
M_f	$U_f/\sqrt{\gamma R T_f}$ reference Mach number
Ma	$uM_f/\sqrt{T}$ Mach number
p	$\rho T/\gamma M_f^2$ pressure of the fluid
Pr	$C_p\mu/\kappa$ Prandtl number
$\vec{Q}$	vector of solution unknowns in physical space
R	gas constant
Re_d	$Re_f \rho_{fd} d_d \lvert\vec{v}_{fd} - \vec{v}_d\rvert$ particle Reynolds number
Re_f	$\rho_f U_f L_f/\mu$ reference Reynolds number
St	t_d/t_f Stokes number
t	time
t_f	L_f/U_f flow time scale
T	temperature
T	flow period
u	velocity of the fluid in x-direction
U_f	reference velocity
v	velocity of the fluid in y-direction

*Assistant Professor, AIAA member, Email: gjacobs@mail.sdsu.edu

v_r	relative particle velocity
x	spatial coordinate in physical space
y	spatial coordinate in physical space

<u>Greek symbols</u>

α	separation angle of the material line
γ	ratio of the specific heats of the fluid
γ	separation location
ϵ	particle to fluid density ratio
κ	thermal conductivity
ρ	density
τ	shear stress
Ω	vorticity

<u>Subscripts</u>

∞	free stream conditions
1	x-direction of τ or the x-plane τ is acting on
2	y-direction of τ or the y-plane τ is acting on
d	particle properties
f	reference variable
fd	carrier-phase properties at particle position
t	derivative with respect to t
x	derivative with respect to x
$-x$	x-direction
y	derivative with respect to y
$-y$	y-direction
$-z$	z-direction

<u>Superscripts</u>

a	advective flux
v	viscous flux

I. Introduction

Particle-laden or droplet-laden separated flows occur in many important natural and technological situations, e.g. aerosol transport and deposition and spray combustion in gas turbine engines. The dispersion, mixing and deposition characteristics of particles greatly affect the optimal circumstances in these environments. Well-mixed fuel droplets, for example, enhance uniform evaporation and effective combustion. A high concentration of particles can pollute the environment. It is thus crucial to understand the particle and droplet behavior.

A number of fundamental dispersion behaviors of inertial particles and droplets are now well established. Inertial particles exhibit a *preferential concentration*[1,2] in flow regions with low vorticity and high strain rate. In turbulent near-wall flows, particles can accumulate in the viscous sublayer.[3–5] Narayan *et al.*[6] showed that particles deposit in near wall flows through either an inertial "free-flight" mechanism or a diffusion mechanism. Tang *et al.*[7] found that if the particle response time is the same as a characteristic flow time, then particles distribute along the periphery of the vortices. An effect that was termed *particle focusing.*

Flow separation has been subject to numerous studies as well (e.g. see Refs. 8 and 9 for reviews). In a recent approach, Haller[10] analyzed flow separation in the Lagrangian frame, i.e. in the frame moving together with fluid particles. He studied the ejection of *massless fluid particles* away from the surface near unsteady flow separation. It was concluded that the fluid particles eject along distinct lines, referred to as "material lines". A flow that *moderately* fluctuates around an averaged flow state features separation of the fluid particles along a material line that emanates from a fixed starting location. This type of separation was termed "fixed unsteady separation". In flows with large (turbulent) fluctuations, the separation location of the material line is better described as moving. The slight off-wall origin (ghost point) of the moving material line can be identified with on-wall data of skin friction and pressure.[11]

Here, we investigate the behavior of finite-sized particles with mass carried in a separating flow as opposed to separation behavior of massless fluid particles. Small and light particles respond fast to the carrier fluid. It can therefor be expected that they separate in a similar manner as the fluid particles. Larger and heavier particles, however, have a slower response to the carrier fluid and their dispersion in fixed and moving separation flows is not trivial. We hypothesize that the unresponsiveness of the fluid particles' ejection location in a fixed separation to a fluctuating flow field is emulated by the even less responsive inertial particles. In moving separating flows, the slow responding inertial particles may well feature fixed separation when the carrier fluid particles' separation is moving. We will test the hypothesis in this paper. To the best of the author's knowledge, no previous studies exist on the inertial particle behavior in separating flows.

We will investigate the inertial particle separation behavior in a two-dimensional transitional flow over a backward-facing step at a Reynolds number of 1500. At this Reynolds number the backward-facing step flow shows a time-dependent periodic shedding behind the step. The averaged flow field is characterized by the well-known recirculation region behind the step, and a corner vortex. The non-trivial averaged separation at the corner vortex sets the ideal stage to study the behavior of particles in an unsteady turbulent-like flow. We will show that particles with Stokes numbers larger than one feature fixed separation.

The outline of this paper is as follows. First, we will briefly present the numerical formulation. Next, we present the computational model followed by a discussion of the unsteady flow separation in the two-dimensional backward-facing step flow. We will then investigate the inertial particle separation behavior in the separated backward-facing step flow. We reserve the final section for conclusions and future work.

II. Formulation and Methodology

For the carrier phase, we consider a compressible and Newtonian fluid, with no bulk viscosity, that is assumed to obey the perfect gas equation of state. The two-dimensional Navier-Stokes equations for the fluid are given, in dimensionless form, by

$$\vec{Q}_t + \vec{F}^a_x + \vec{G}^a_y = \frac{1}{Re_f}(\vec{F}^v_x + \vec{G}^v_y), \tag{1}$$

where

$$\vec{Q} = \begin{bmatrix} \rho \\ \rho u \\ \rho v \\ \rho e \end{bmatrix}, \quad \vec{F^a} = \begin{bmatrix} \rho u \\ p + \rho u^2 \\ \rho uv \\ u(\rho e + p) \end{bmatrix}, \quad \vec{G^a} = \begin{bmatrix} \rho v \\ \rho uv \\ p + \rho v^2 \\ v(\rho e + p) \end{bmatrix}. \tag{2}$$

The energy flux, e, is defined using the ideal gas relation as $\rho e = p/(\gamma - 1) + \rho(u^2 + v^2)/2$ where $\gamma = 7/5$. The viscous fluxes are expressed as

$$\vec{F^v} = \begin{bmatrix} 0 \\ \tau_{11} \\ \tau_{21} \\ u\tau_{11} + v\tau_{21} + \frac{1}{(\gamma-1)M_f^2 Pr} T_x \end{bmatrix}, \quad \vec{G^v} = \begin{bmatrix} 0 \\ \tau_{12} \\ \tau_{22} \\ u\tau_{12} + v\tau_{22} + \frac{1}{(\gamma-1)M_f^2 Pr} T_y \end{bmatrix}, \tag{3}$$

where, under the Stokes hypothesis, the shear stresses are given by

$$\begin{aligned} \tau_{11} &= 2[u_x - (u_x + v_y)/3], \\ \tau_{22} &= 2[v_y - (u_x + v_y)/3], \\ \tau_{12} &= v_x + u_y. \end{aligned} \tag{4}$$

The subscript on the stress tensor, τ, defines the direction of τ and the plane it is acting on, where 1 and 2 denote the x and y direction, respectively. The equation of state is $p = \rho T/\gamma M_f^2$. All of the variables are normalized by reference length (L_f), density (ρ_f), velocity (U_f), and temperature (T_f) scales. The reference Reynolds and Mach numbers are defined by $Re_f = \rho_f U_f L_f/\mu$ and $M_f = U_f/(\gamma R T_f)^{1/2}$, respectively, and the Prandtl number is $Pr = C_p\mu/\kappa$.

The particles are assumed spherical. A one-way coupling between the carrier phase and the particle phase is assumed, i.e. the effect of the particles on the carrier phase is neglected. The particles are tracked individually in a Lagrangian manner, with the instantaneous particle position and velocity given by $\vec{x}_d$ and $\vec{v}_d$. The Lagrangian equations for particle position and velocity, non-dimensionalized with U_f and L_f, are given by[12]

$$\frac{d\vec{x}_d}{dt} = \vec{v}_d, \tag{5}$$

$$\frac{d\vec{v}_d}{dt} = \frac{C_{Ds}}{St}(\vec{v}_{fd} - \vec{v}_d) + C_A \frac{1}{\epsilon}\frac{d}{dt}(\vec{v}_{fd} - \vec{v}_d) + \frac{1}{\epsilon}\frac{D(\vec{v}_{fd})}{Dt} + \frac{0.2C_H}{(\epsilon St)^{1/2}} \int_{t_0}^{t} \frac{d(\vec{v}_{fd} - \vec{v}_d)/d\tau}{\sqrt{t-\tau}} d\tau + \frac{0.727}{(\epsilon St|\vec{\Omega}|)^{1/2}} \begin{bmatrix} (v_{fd-y} - v_{d-y})\Omega_{-z} \\ -(v_{fd-x} - v_{d-x})\Omega_{-z} \end{bmatrix}, \tag{6}$$

where

$$\frac{D}{Dt} = \frac{\partial}{\partial t} + v_{fd-x}\frac{\partial}{\partial x} + v_{fd-y}\frac{\partial}{\partial y}, \tag{7}$$

and

$$\frac{d}{dt} = \frac{\partial}{\partial t} + v_{d-x}\frac{\partial}{\partial x} + v_{d-y}\frac{\partial}{\partial y}. \tag{8}$$

Equation (6) is the so-called Basset-Boussinesq-Oseen (BBO) equation. The terms on the right-hand side represent, in order, the effects of the steady state drag, the virtual mass force, the pressure drag, the Basset history force and the Saffman lift force.

In (6), $\vec{\Omega} = \nabla \times \vec{v}_{fd}$, represents the vorticity of the carrier phase and $\epsilon = \rho_d/\rho_{fd}$ is the ratio of the particle to fluid density. The Stokes number is defined as

$$St = \frac{t_d}{t_f} = \frac{{d_d}^2 \rho_d Re_f}{18}, \tag{9}$$

where t_d represents the particle response time and t_f is a characteristic flow time, defined here as the ratio of the step height of the backward-facing step to the free-stream velocity.

With the following empirical correction factors the equations are accurate for $Re_d < 1000$,

for the Stokes drag,[12]

$$C_{Ds} = 1 + \frac{{Re_d}^{2/3}}{6}, \tag{10}$$

$$C_A = 1.05 - \frac{0.066}{{A_c}^2 + 0.12}, \tag{11}$$

for the virtual mass force,[13] and

$$C_H = 2.88 + \frac{3.12}{(1 + A_c)^3}, \tag{12}$$

for the Basset history force.[13] Here, A_c represents the relative acceleration factor defined as

$$A_c = \frac{{v_r}^2/d_d}{dv_r/dt}, \tag{13}$$

where v_r is the relative particle velocity.

The carrier phase is solved with a multidomain Chebyshev spectral method. The method has been described and tested extensively in our previous papers[14–16] so for brevity will not be explained here. We track particles with the tracking algorithm developed in Ref. 17. The algorithm uses a second order Adams-Bashforth scheme for time integration of the particle equations. A sixth order Lagrangian scheme interpolates the carrier phase variables to the particle position.

III. Backward-Facing Step: Carrier Flow

We compute the two-dimensional compressible, transitional flow over an open-backward facing step. We choose this flow, since it features the non-trivial, unsteady, strongly fluctuating separation, in which we aim to investigate inertial particle dispersion. Moreover, the benchmark backward-facing step flow is well documented[18–21] setting a reliable stage for the particle investigation.

A. Computational Model

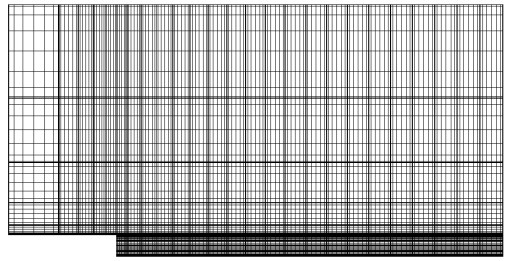

Figure 1. Computational model and grid over a backward facing step.

We consider the non-confined or open backward-facing step flow at a Reynolds number of, Re_f=1500 based on the step height and the inflow velocity, and a Mach number of Ma=0.4 based on the inlet velocity and the isothermal wall temperature. In Jacobs[18] this flow was studied extensively in 2D and 3D. We refer to this reference for a detailed description of the simulation and a convergence study.

To summarize: the computational domain and grid are shown in Figure 1. The grid consists of 180 domains. On each subdomain a tenth order approximation of the Navier-Stokes equation is projected using a nodal basis. The computational domain size is chosen to ensure a minimal blockage of the top inflow. At the left inflow boundary a uniform velocity is specified, while at the right outflow boundary a velocity profile is specified according to an experimental averaged turbulent boundary layer. The wall boundary conditions are no-slip and isothermal. The flow is initialized with the uniform inlet velocity.

B. Flow topology

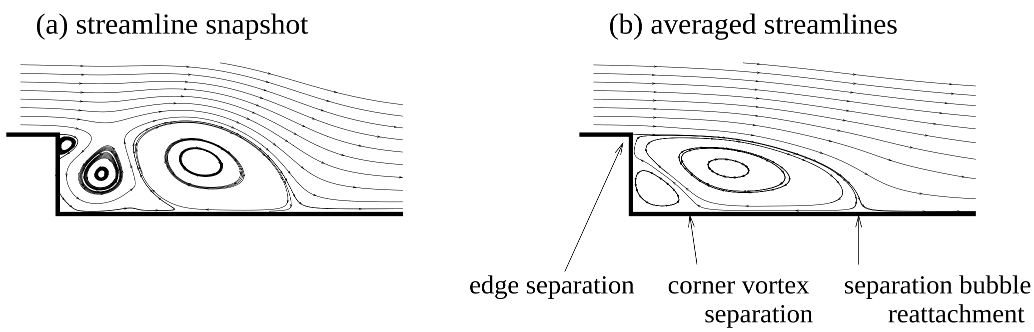

Figure 2. Instantaneous (a) and averaged (b) streamlines of the 2D flow over a open backward-facing step at Reynolds number, Re_f=1500 and Mach number Ma=0.4. The instantaneous streamlines show a complex vortex shedding pattern of this flow. If averaged the streamline pattern exhibits a typical recirculation with edge and corner vortex separation, and a shear layer reattachment.

After an initial flow development, the two-dimensional backward-facing step flow exhibits a periodic shedding of a three-vortex system behind the step.[19] First, a vortex forms near the corner of the step. This vortex grows in strength and size as it is fed by the external flow. With increasing strength the vortex increasingly pushes itself away from the wall, until it sheds off. The shedding occurs in an intimate three vortex interaction between the vortex at the step, the corner vortex behind the step, and the shedded vortex (Fig. 2a).

The averaged flow pattern is quite regular with a typical recirculation region behind the step (Fig. 2b) . A corner vortex is also present behind the step in the averaged flow field. The flow separation at the sharp edge of the step is trivial. The shear layer that emanates from the step corner reattaches behind the step. A *non-trivial* flow separation is found on the lower wall behind the step between the corner vortex and the recirculation.

C. Corner Flow Separation: Fluid Particles

The corner vortex separation location in the averaged flow field as indicated in Fig. 2b coincides with a zero averaged skin friction point on the bottom wall. The instantaneous Eulerian separating streamline induced by the unsteady corner vortex dynamics with a start location at the zero wall skin friction point, is unsteady and fluctuates quite severely. In this type of unsteady separating flow with an asymptotic mean, the instantaneous fluid particle separation in the Lagrangian frame is fixed,[10, 22] i.e. fluid particles separate from the averaged zero skin friction location into sharp time-dependent material lines. The separation angle of the material line with the wall is time-dependent (Fig. 3a), and the ejection direction of the fluid particles away from the wall is unsteady. The separation angle is theoretically determined with the time-history of the skin friction and wall pressure at the separation location, γ, as

$$\tan\alpha(t_0) = \frac{\lim_{T\to-\infty} -3\frac{1}{T}\displaystyle\int_{t_0}^{T} \tau_x(\gamma,t)\ dt}{\lim_{T\to-\infty} \frac{1}{T}\displaystyle\int_{t_0}^{T}\left[p_x(\gamma,0,t) + 3\tau_x(\gamma,t)\int_{t_0}^{t}(1/\mu)\tau(\gamma,t)ds\right]\ dt}. \tag{14}$$

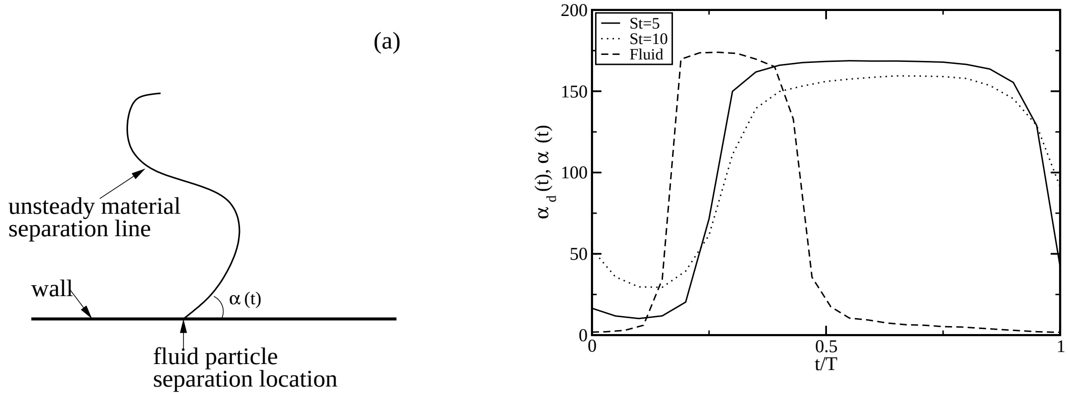

Figure 3. Schematic of a material line formed by particles separating from a wall (a). Separation angle of fluid particles $\alpha(t)$ and inertial particles, $\alpha_d(t)$, versus time at the unsteady corner vortex separation location in the quasi-steady backward-facing step flow over one flow period.

The temporal development of fluid particles traced in the Eulerian flow field confirms (not shown here) that the fluid particles separate from a fixed location. They do so, however, under very small angles in this strongly fluctuating separating flow. Fig. 3b shows that the separation angle is mostly near 0 or 180 degrees in one flow period. Fluid particles thus predominantly eject away nearly parallel to the wall. Further away from the fixed separation location fluid particles reach into the flow (Fig. 4a) and form lines whose off-wall origin is moving with the shedded vortex (Fig. 4b and c). When fluid particles separate like this, the separation location is better identified by the moving off-wall location of the the fluid particle line than the fixed separation location. The moving location can be estimated theoretically with the wall-based criteria proposed in Ref. 11. Moving separation can be expected in flows that feature an onset of separation or a quasi-steady separation with strong turbulent flow fluctuations. The corner separation is of the second type.

IV. Inertial Particle Separation in the Unsteady Corner Vortex Separation

Inertial particles have a delayed response to the flow as compared to fluid particles. This will naturally have an affect on the separation of these particles as compared to fluid particle separation. Here, we study the effect of inertia on the particles' dispersion in the unsteady corner separating flow discussed in the previous section. We first track particles that only have a Stokes drag acting upon them. Later we determine the effect of other forces in the BBO equation (6) on the particle dispersion.

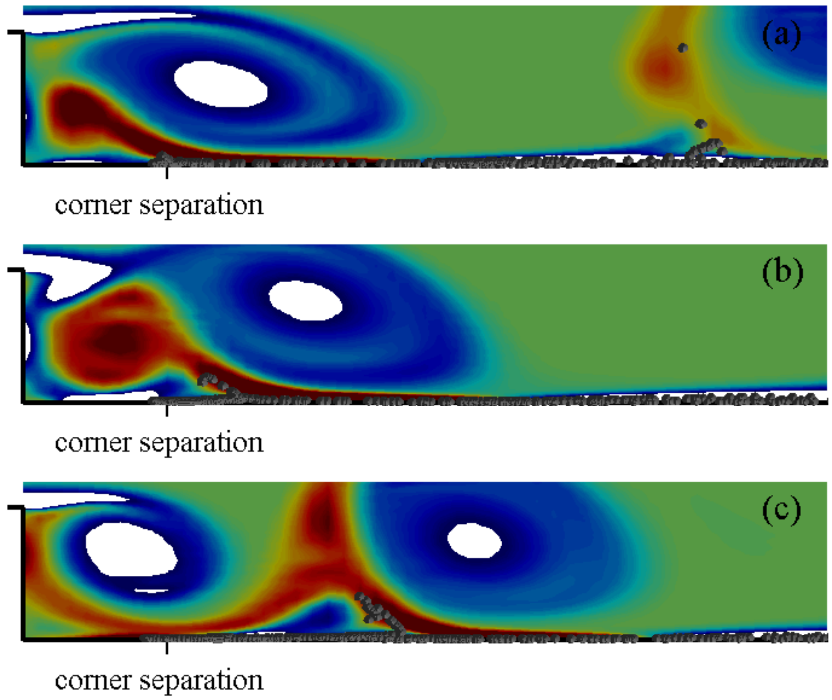

Figure 4. Fluid particles and vorticity contours at three equi-spaced consecutive times within a flow period in the quasi-steady backward-facing step flow. The fluid particles are continuously injected near the corner separation location. Material lines form at the corner separation location and move with the shedded vortex downstream into to the flow.

A. Stokes Drag

To start, we consider particles that are affected by only the Stokes drag. Inertial particles are continuously released near the wall with a zero initial velocity at the fixed fluid particle corner vortex separation location. Their paths are then traced in time in the computed Eulerian backward-facing step carrier flow.

We consider particles with four different Stokes numbers, including St=0.1, 1, 5 and 10. The Stokes number (as defined in (9)) compares the response time of the particles, which is dependent on the particle's density and size, to a characteristic time scale of the carrier flow. In the backward-facing step flow, the characteristic time scale is chosen the ratio of the step height to the free-stream velocity. At St=0.1 the particle response time is one order of magnitude smaller then the flow time scale. The particles thus respond quickly to changes in the carrier fluid and the inertial particle dispersion is, therefore, expected to closely follow the fluid particle traces. At St=1 the flow time and particle time scale are the same, and the inertial particle dispersion is not easily predicted. At further increasing Stokes number the particles will respond slower to the carrier flow.

The particles' dispersion at St=0.l (Fig. 5b) indeed follows the moving separation of the massless fluid particles(Fig. 5a). Close to the wall, the inertial particles separate at the zero averaged skin friction location at small angles. The inertial particles eject into a line that moves along with the shedding vortex. A notable difference with the moving fluid material line is that the inertial particle material line does not extend as far away from the wall. The inertial particles' respond slower than the fluid particles to the carrier flow upwelling at the separation location and are therefore not ejected as as far into the domain.

At St=1 (Fig. 5c) the particle material line is no longer moving. The particles stay very near the wall close the fixed fluid separation location. They periodically eject and retreat responding to the upwelling of a shedded vortex followed by the downwelling of the corner vortex that is induced by the shedded vortex. The vortex system so traps the particles at the separation location.

At Stokes number larger than one (Fig. 5d,e), the inertial particle dispersion is very similar to the fixed

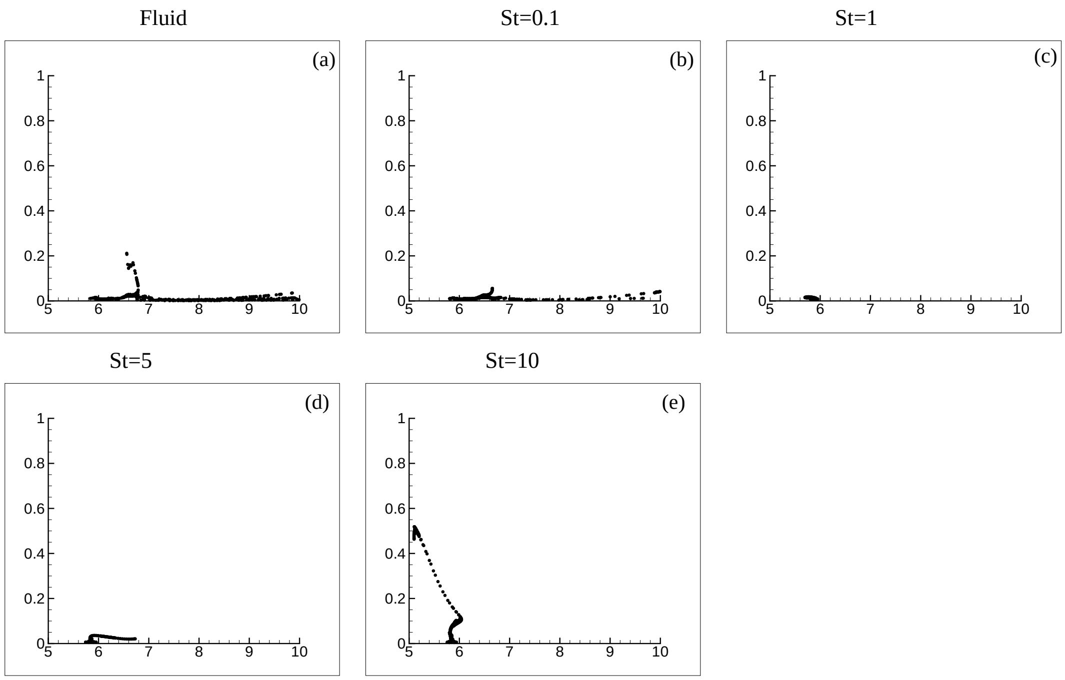

Figure 5. The separation material line formed by fluid particles (a), and inertial particles with St=0.1 (b), St=1 (c), St=5 (d), and St=10 (e). The separation line changes from a "moving separation" line at $St < 1$ to a "fixed separation" line at $St > 1$.

unsteady fluid particle separation. The particles eject from the averaged zero skin friction location into a sharp material line. The ejection angle of the particles and the material line shape is time-dependent. With increasing Stokes number the separation angle is steeper and the amplitude of oscillation of the material line reduces. At very large Stokes number (not shown) the particles eject along a fixed trajectory that initially aligns with the averaged separating carrier flow streamline (Fig. 2b).

The particle separation angle, $\alpha_d(t)$, determined from the particle material line, plotted versus time within a period in Fig. 3b shows that the separation angle is not only increasing with the increased inertia. It also shows that the separation angle is increasingly out of phase with the fluid particle separation angle. We can understand the phase lag from the temporal development of the carrier flow vorticity and the particle material line as shown in Fig. 6: The inertial particle line near the wall is forced by a counter-clockwise vortex (red vorticity contour in Fig. 6a) that is shed downstream. The carrier flow forcing first decelerates the motion of the particle line in negative x-direction and consequently accelerates the particle line in positive x-direction(Fig. 6b). When the particle line moves in positive direction, the counter-clockwise vortex is shed downstream and the large recirculating clockwise rotating vortex is at the particle location (Fig. 6c). The carrier velocity then is negative near the wall and hence forces the material line back. Since the particle line moves in negative x-direction when the carrier velocity and the fluid particle motion is in positive x-direction and vice-versa, the inertial particle separation angle is out of phase with the fluid particles separation angle. With increased Stokes number the response time is slower and the phase lag increases.

In summary, particles with a Stokes number smaller than one exhibit a moving separation similar to the moving fluid particle separation, whereas particles with a Stokes numbers larger than one separate in a fixed manner. To the best of the author's knowledge, both these behaviours are not documented.

B. BBO-forces

In the previous section we only considered the influence of Stokes drag on the particle trajectories. For large densities of the particle (ϵ >1000) this is typically the only significant force on spherical particles. Forces other then the Stokes drag may, however, be significant in unsteady flows with large shear such as the unsteady near wall flow at the corner separation.

Comparison of the separation line computed with only the Stokes drag influence (Fig. 7a) and the full

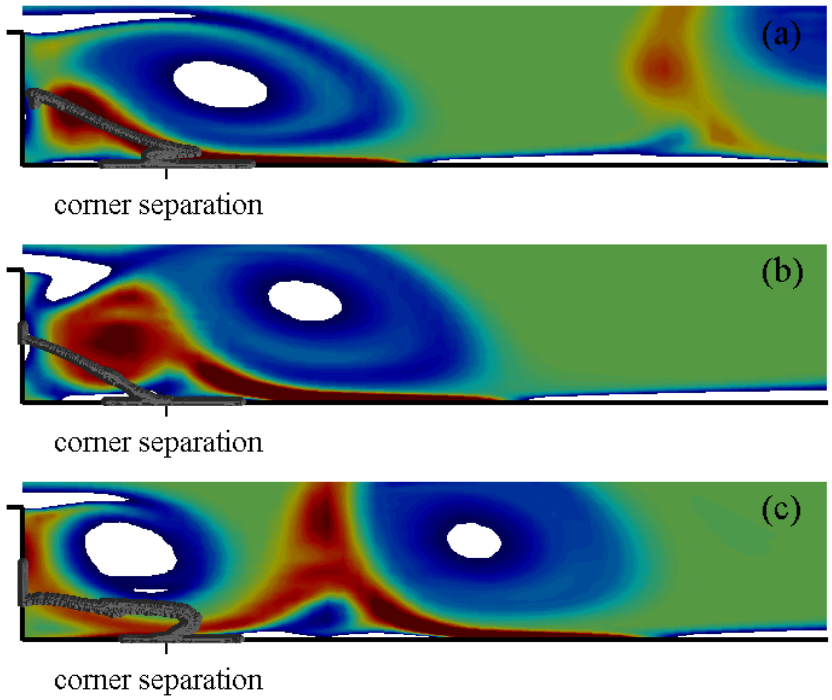

Figure 6. Same as Fig. 4, but the particles are finite-sized with St=10. The inertial particles separate from the fixed averaged zero skin friction location.

BBO equation (Fig. 7b) at ϵ=1000 shows a significant effect. First, the material line is not quite as distinct with BBO as it is with Stokes and particles are dispersed to locations other then the material line. The material line stays clearly visible, since the bulk of the particles are close to the material line. The nature of the particle separation is still fixed, but the shape of the material line has changed.

From Fig. 8, which plots the contributions of the separate forces in the BBO equation for one particle trace with St=10 and ϵ=1000, we learn that the Saffman lift is responsible for the changes in the particle separation. Most forces other than the Stokes drag are negligible as expected for this high particle to fluid density ratio. The high shear velocity layer near the wall, however, leads to a significant Saffman lift on the particle in wall normal direction. The lift force results in an increased particle ejection that changes the material line. The lift force is large throughout the near wall region, and therefore particles eject away from the wall at locations other then the fixed separation location. This particle ejection in regions other then the fluid particle separation location pollutes the sharpness of the material line determined with only the Stokes drag. Since the Saffman lift is approximately five times smaller than the large Stokes force on the particle, the particle material line formed due to the Stokes force is still clearly visible.

V. Conclusion and Future Work

We have identified that inertial particles separate from a fixed location in a quasi-turbulent unsteady separating flow with an asymptotic mean, where the fluid particle separation is moving. Inertial particle separation is fixed for particles whose response time is larger than the characteristic flow time scale. At increasing Stokes number the time-dependent separation angle of the inertial particles increases and it is also increasingly out of phase with the fluid particle separation angle.

If the response time is smaller than the characteristic flow time, the inertial particle separation compares to the moving fluid particle separation.

If the flow and particle time scales are the same, inertial particles are trapped at the separation location.

The Saffman lift may be significant in unsteady separating flows. If it is, the Saffman lift ejects particles

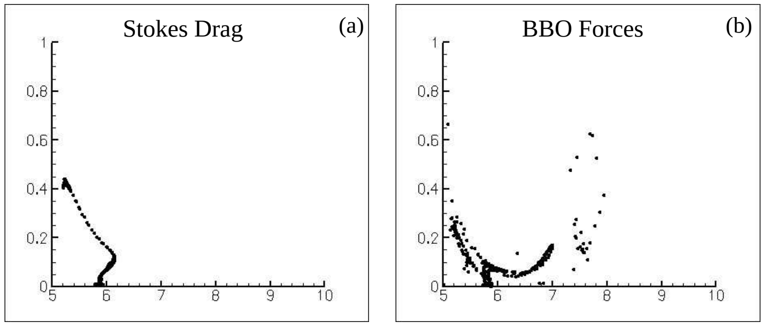

Figure 7. The material separation line for particles that are traced with only the Stokes force (a), and with the BBO equation (b)at ϵ=1000.

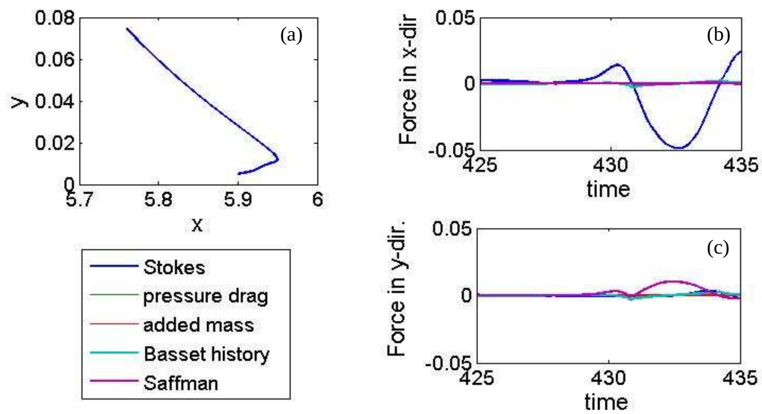

Figure 8. The particle trace in the x and y plane determined with the BBO equation (a). The force components of the BBO equation in x-direction and y-direction, including the Stokes drag, pressure drag, added mass force, Basset history, and Saffman lift.

away from the wall at locations other than the averaged zero skin friction location. The separation material line is then less sharp. The bulk of the particles are, however, still following the Stokes material line separation.

Current efforts focus on the identification of fixed inertial particle separation behavior in three dimensional separating flows.

Acknowledgments

The University Grant Program at San Diego State University partially sponsored this research.

References

[1] Wang, L.-P. and Maxey, M. R., "Settling velocity and concentration distribution of heavy particles in isotropic turbulence," *J. Fluid Mech.*, Vol. 256, 1993, pp. 27–68.

[2] Squires, K. D. and Eaton, J. K., "Particle response and turbulence modification in isotropic turbulence," *Phys. Fluids*, Vol. 2, 1990, pp. 1191–1203.

[3] McLaughlin, J. B., "Aerosol particle deposition in numerically simulated channel flow," *Phys. Fluids*, Vol. 1, 1989, pp. 1211–1224.

[4] Brooke, J. W., Kontomaris, K., Hanratty, T. J., and McLaughlin, J. B., "Turbulent deposition and trapping of aerosols at a wall," *Phys. Fluids*, Vol. 4, No. 4, 1992, pp. 825–834.

[5] Brooke, J. W., Hanratty, T. J., and McLaughlin, J. B., "Free-flight mixing and deposition of aerosols," *Phys. Fluids*, Vol. 6, No. 10, 1994, pp. 3404–3415.

[6] Narayan, C., Lakehal, D., Botto, L., and Soldati, A., "Mechanisms of particle deposition in a fully developed turbulent open channel flow," *Phys. Fluids*, Vol. 15, Mar. 2003, pp. 763–775.

[7] Tang, L., Wen, F., Yang, Y., Crowe, C. T., Chung, J. N., and Troutt, T. R., "Self-organizing particle mechanism in a

plane wake," *Phys. Fluids A*, Vol. 4, Oct. 1992, pp. 2244–2251.

[8] Schlichting, H. and Gersten, K., *Boundary-Layer Theory.* Springer., 8th ed., 2000.

[9] Delery, J. M., "Robert Legendre and Henri Werle: Toward the elucidation of three-dimensional separation," *Ann. Rev. Fluid Mech.*, Vol. 33, 2001, pp. 129–154.

[10] Haller, G., "Exact theory of unsteady separation for two-dimensional flows," *J. Fluid Mech.*, Vol. 512, 2004, pp. 357–311.

[11] Surana, A. and Haller, G., "Ghost manifolds in slow-fast systems, with application to unsteady fluid flow separation," *Physica D*, 1007. in press.

[12] Crowe, C. T., Sommerfeld, M., and Tsuji, Y., *Multiphase Flows with Droplets and Particles.* Boca Raton, Fl: CRC Press LLC, 1998.

[13] Odar, F. and Hamilton, W. S., "Forces on a Sphere Accelerating in a Viscous Fluid," *J. Fluid Mech.*, Vol. 18, 1964, pp. 302–314.

[14] Kopriva, D. A., "A staggered-grid multidomain spectral method for the compressible Navier-Stokes equations," *J. Comp. Phys.*, Vol. 143, 1998, pp. 125–158.

[15] Jacobs, G. B., Kopriva, D. A., and Mashayek, F., "A particle-tracking algorithm for the multidomain staggered-grid spectral method," AIAA Paper 2001-0630, 2001.

[16] Jacobs, G. B., Kopriva, D. A., and Mashayek, F., "Outflow Boundary Conditions for the Multi-Domain Staggered-Grid Spectral Method for the Navier-Stokes Equations," AIAA Paper 2002-0903, 2002.

[17] Jacobs, G. B., Kopriva, D. A., and Mashayek, F., "Towards efficient tracking of inertial particles with high-order multidomain methods," *J. Comp. Appl. Math.*, Vol. 206, 2007, pp. 293–408.

[18] Jacobs, G. B., *Numerical Simulation of Two-Phase Turbulent Compressible Flows with a Multidomain Spectral Method.* PhD thesis, University of Illinois at Chicago, 2003.

[19] Le, H. and Moin, P., "Direct simulations of turbulent flow over a backward-facing step," Department of Mechanical Engineering Report TF-58, Stanford University, Stanford, CA, 1994.

[20] Jovic, S. and Driver, M., "Backward-facing step measurements at low Reynolds number, Re_h=5000.," NASA TM 108807, Feb. 1994.

[21] Wengle, H., Huppertz, A., Barwolff, G., and Janke, J., "The manipulated transitional backward-facing step flow: an experimental and direct numerical investigation.," *Eur. J. Mech. B - Fluids*, Vol. 20, 2001, pp. 25–46.

[22] Weldon, M., Peacock, T., Jacobs, G., Helu, M., and Haller, G., "Experimental and numerical investigation of the kinematic theory of unsteady separation," *J. Fluid Mech.*, 2007. submitted.